

# Scanline survey to characterize outcrops and excavation faces of ancient quarries in urban area: a case study of Meknes city, Morocco

Abdelouahed Essaied <sup>1\*</sup>, and Mohamed Rouai<sup>1</sup>

<sup>1</sup>Moulay Ismail University, Faculty of Sciences, PO Box 11201 Zitoune, Meknes, Morocco

**Abstract.** The analysis of rock outcrop fracturing and excavation faces in urban areas is important to evaluate their stability. Meknes region, in Northern Morocco, contains several limestone quarries, making it a good location for this study. Two sites were investigated using the Scanline technique, which allows to the identification, mapping, and characterization of discontinuities. The results highlight three fracture sets oriented N45, N110, and N80, conforming the dominant orientations of regional fracturing. The analysis also reveals that the distribution of spacing, apertures, and persistence of the discontinuities is random. In terms of filling, most discontinuities are closed or moderately open without any filling, although, silt or red soil deposits are occasionally observed.

**Keywords:** Urban geology, risk, discontinuity, scanline survey.

## 1 Introduction

In urban areas, human activities have a significant impact on the stability of rock outcrops and excavation faces. Waltham and Fookes (2003) [1], report that anthropogenic vibrations caused by railway traffic or proximal construction work can de-stabilize slopes and increase the risk of rockfalls or collapses. Furthermore, Piteau and Martin (1977) [2] underline that discontinuities, such as fractures, faults, and joints, play an essential role in slope stability by influencing their mechanical behavior.

The excavation faces of ancient limestone quarries and other rock outcrops in Meknes region are exposed to weather conditions and seismotectonic events, which can reduce their stability over time [3]. This instability put the historical monuments and infrastructures in risk. To confront these challenges, a fracture analysis was applied using the Scanline method. This technique characterizes rock outcrop discontinuities by examining parameters such as orientation, spacing, aperture, and persistence [4]. This data are essential for evaluating and assessing the state of fracturing and its impact on the stability of the studied outcrops [5].

---

\* Corresponding author: [author@email.org](mailto:author@email.org)

The research aimed on describing statistical histograms and mapping discontinuity attributes, determining their principal characteristics, and linking this discontinuities system to the regional structural context across two sites in the study area.

The obtained results will provide a reference for evaluating outcrop stability, facilitating quarry restoration and enhancing risk assessment practices.

## 2 Geological and structural context

Located in the western part of the Saïs Basin (Fig. 1). The urban area of Meknes is bounded to the North by the South Rifain Ridges, primarily composed of Mesozoic materials [6], and to the South by the Tabular Middle Atlas (TMA), composed of fractured Liassic limestone and dolomite [7]. The Saïs Basin is predominantly made up of thick Miocene marls, reaching 900m in the northeast and unconformably over-laying Liassic deposits [8]. These marls are characterized by a high degree of consolidation regarding their mechanical behavior [9].

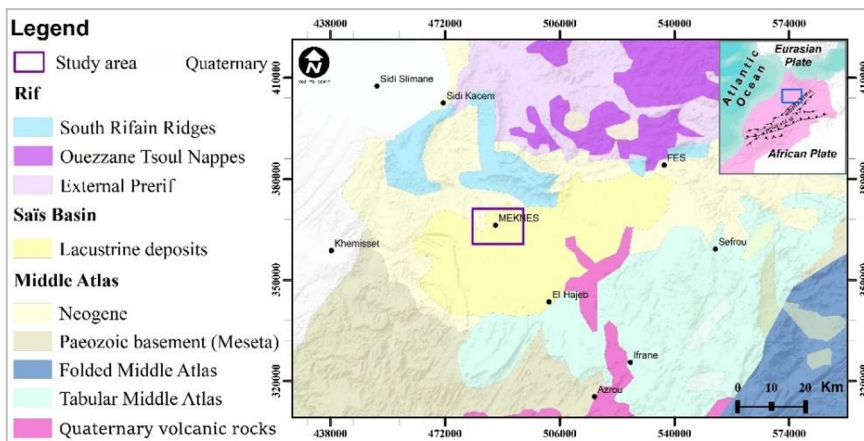


**Fig. 1.** Geological context of the study area [6].

From structural framework, the study area exhibits numerous flexures with a dominant NE-SW to NNE-SSW orientation, resulting in a stepped topographic structure dipping towards the NW (Fig. 1). These flexures are an extension of the major structural lineaments associated with the central Paleozoic massif [10]. The region is bounded to the North by a thrust sheet formed during a N-S compressive phase [11], and to the South by a fractured tabular structure (TMA) influenced by major NE-SW faults [12].

Geologically, the area is dominated by altered lacustrine limestone, accompanied by outcrops of hard limestone in several locations [7]. Valley bottoms are primarily composed of marls, with local occurrences of sands in specific location [13]. The marl deposits are exposed at the surface in the north of the urban area [14]. The general geologic map is presented in Fig. 2B.



### 3.2 Variographic analysis

The application of the MatterCliff software enabled the computation of variograms in accordance with the approach proposed by Matheron (1969) [17], in order to better describe the spatial distribution of fracture spacing and analyze their cluster-ing.

Variographic analysis is frequently used for the analysis of geological discontinuities. The variogram  $\Gamma(h)$  is constitutes a powerful statistical tool, particularly in the study of fracturing in rock mechanics [18]. It is defined by the following equation:

$$\Gamma(h)=1/2 \text{ VAR}[Z(x+h)-Z(x)] \quad (1)$$

$\Gamma(h)$  is the semi-variogram ( $2\Gamma(h)$  is the variogram),  $h$  is the lag, and  $\text{VAR} [Z(x)]$  is the variance at point  $x$ .

The variogram is characterized by the intercept, the range, and the sill (Fig. 4). A non zero intercept is known as the nugget effect. The range defines the limit distance beyond which spatial data present no correlation, while the sill reflects the variance value outside the correlation zone Matheron (1969) [17].

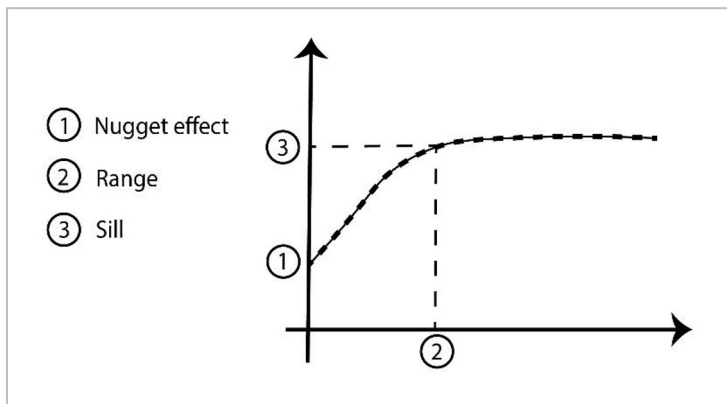


Fig. 4. Variogram with nugget effect.

### 3.3 Data

Two sites were selected within the urban area of Meknes: an outcrop in the Toulal sector (site 1), and the rock faces from an abandoned quarry located in Kortoba sector (site 2). Geologically, these sites consist of Pliocene lacustrine limestone, as indicated by Cirac, (1985) [19]. They appear as horizontal layers with thickness ranging from 0.5 to 2 meters. At these sites, measurements were carried out 1.5 meters above the natural ground level along a horizontal line.

A two-dimensional (2D) observation face were established by taking a series of photos with a 5 meter distance between the photographer and the studied outcrop, measured using a laser distance meter.

The image stitching allows for a panoramic view of the outcrop. Subsequently, all observed discontinuities were digitized for quantification and analysis for each site (Fig. 5)

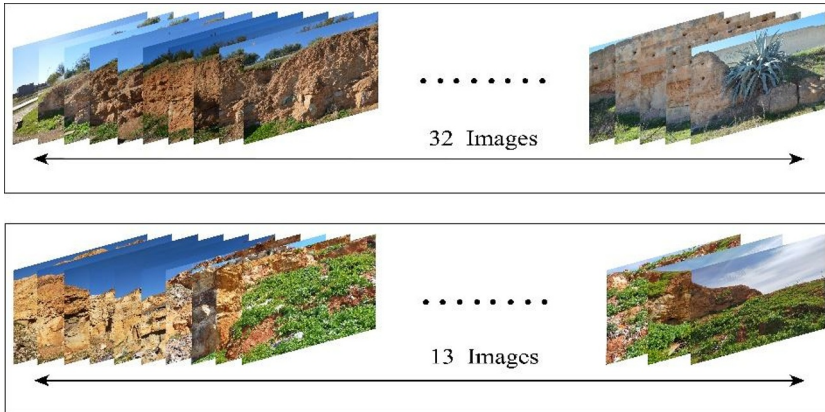


**Fig. 5.** Image stitching for scanline mapping

## 4 Results and discussion

### 4.1 Discontinuity survey

At site 1, 36 discontinuities were identified and measured. At site 2, 20 were sampled along the excavation face. Visually, site 2 shows more compact materials than site 1 (Fig. 6).

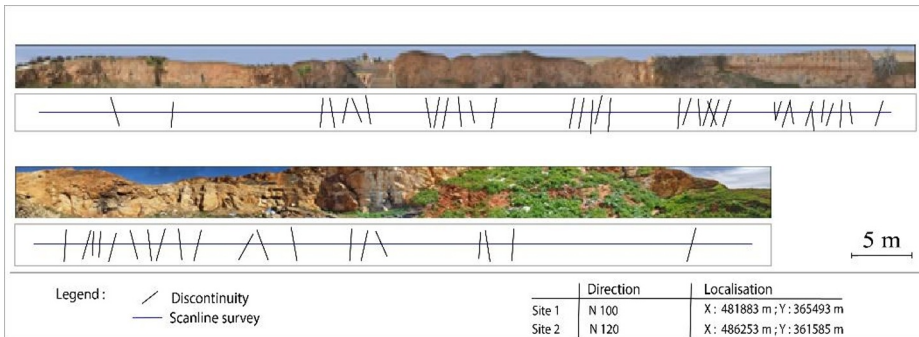


**Fig. 6.** Scanline survey.

### 4.2 Orientation

The analysis shows that the dominant fracture family at site 1 is oriented ENE-WSW, with two secondary families, ESE-WNW and NE-SW. Site 2 is characterized by a single dominant family, oriented NNE-SSW.

At two sites, the discontinuities are vertical to subvertical. The directional rose diagrams show the distribution of discontinuities orientations (Fig. 7).

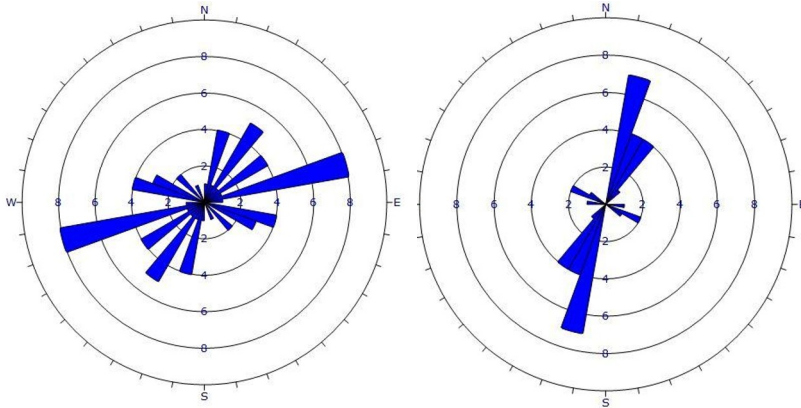


**Fig. 7.** Rose diagram.

### 4.3 Analysis of discontinuity spacing

#### Frequency histogram

The spacing is defined as the average distance between two consecutive discontinuities along a direct line. This parameter is important for evaluating the density of cracks or fractures within the rock mass [15].

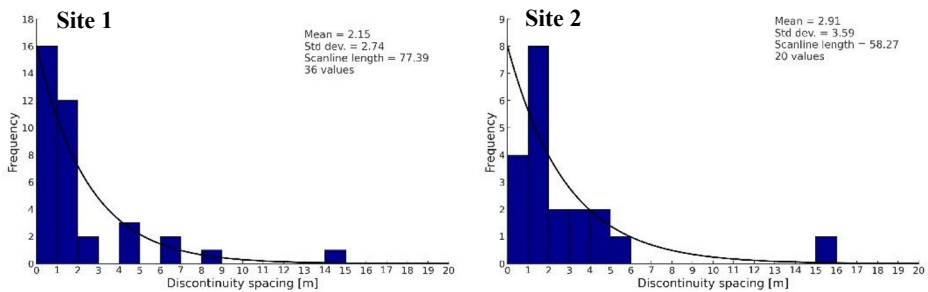


**Fig. 8.** Histograms of discontinuity spacing.

The spacing distribution of discontinuities within the dominant families at the studied sites (Fig. 8) follows a negative exponential law, indicating a random distribution [20].

The analysis of discontinuity spacing across the two sites revealed various observations. At site 1, the average spacing is 2.1 m with a standard deviation of 2.7 m. However, site 2 shows an average of 2.9 m and a standard deviation of 3.6 m.

The discontinuity spacing across the sites shows a rapid decrease, suggesting that shorter distances are more frequent.

#### Variographic analysis

In general, a flat variogram reflects a random distribution of data, while an irregular curve indicates a non-random.

The variograms of the two sites (Fig. 9) show low variations in the spatial distribution of discontinuities.

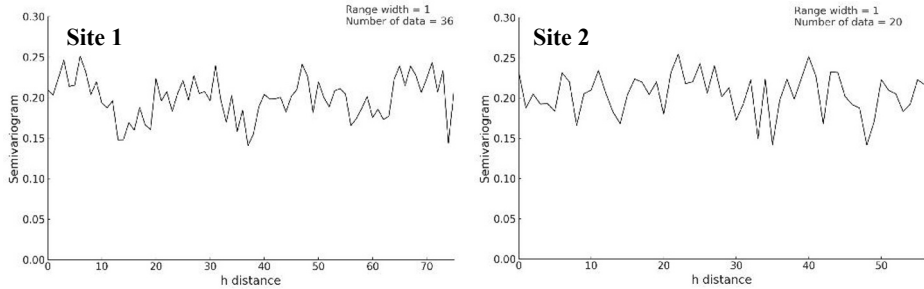


**Fig. 9.** Variograms of discontinuity spacing.

The variograms are relatively flat, suggesting a random distribution of discontinuity spacings, confirming the results obtained from the histograms.

#### 4.4 Analysis of discontinuity apertures

The histograms of discontinuity apertures for the two sites emphasize clear distinctions. The site 1 shows an average aperture of 7.4 cm with a standard deviation of 7.8 cm. In contrast, site 2 shows the average aperture at 2.8 cm, with a standard deviation of 4.3 cm (Fig. 10). The histograms show that the majority of fracture apertures are less than 10 cm across the two sites, with a frequency that decreases rapidly at low values.

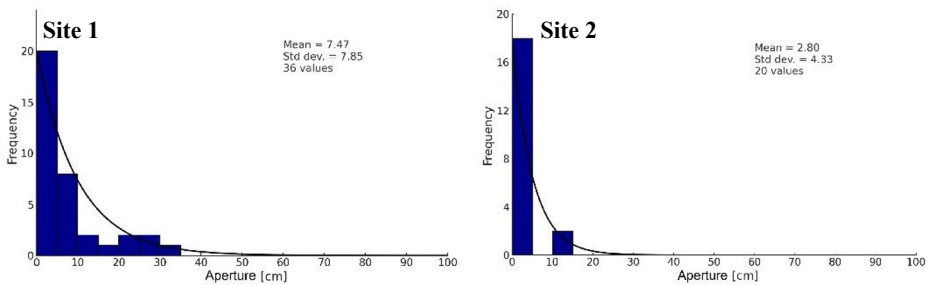


**Fig. 10.** Histograms of discontinuity apertures.

The distribution follows a negative exponential law, indicating a random distribution of apertures. The differences in the mean apertures (ranging from 2.79 cm to 7.85 cm) reflect local variability in the geological conditions of the sites. At site 1, over 56% of the apertures measure less than 5 mm. In contrast, only 10% of the apertures at site 2 exceed 5 mm, revealing inter site variability in aperture sizes. The fractures with apertures greater than 10 mm in site 1 represent 22%. Conversely, site 2 present lower proportions, with only 10% of the fractures exceeding 10 mm (Fig. 10).

#### 4.5 Filling of discontinuity apertures

In general, the properties of the filling material influence the shear strength, deformability, and permeability of the discontinuities [15]. Two types of filling materials are identified, soft and hard materials [15].

In this study, at site 1, over 8% of the fractures are filled with silts, rising to 20% at site 2. The Figure 11 illustrates a typical example of a fracture filled with silty material.

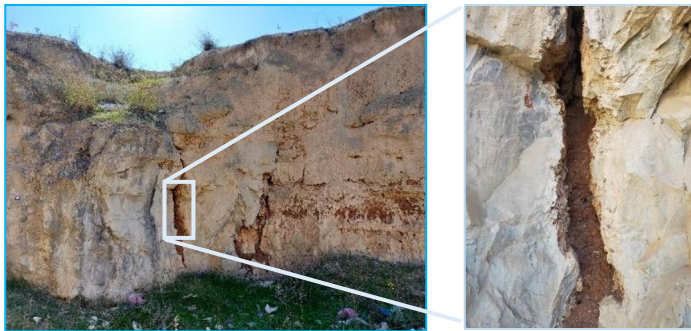


**Fig. 11.** Typical example of a discontinuity filled with silt material.

#### 4.6 Persistence of discontinuities

The discontinuity lengths across the two sites indicate that most discontinuities are less than 1.5 meter long, with the frequency decreasing rapidly for greater lengths (Fig. 12).

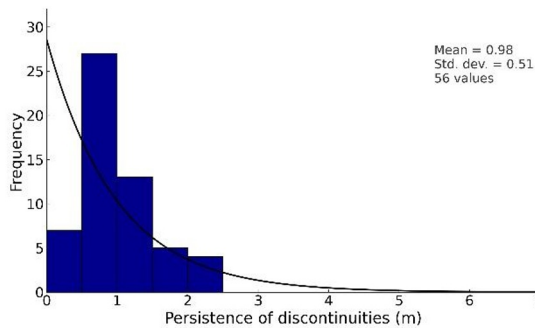


**Fig. 12.** Histograms of discontinuity persistence.

This distribution is distinctly asymmetrical, following a negative exponential law, reflecting a random distribution of persistence [20].

The average length of the discontinuities recorded at both sites is 0.98 m, ranging from 0.40 m to 2.43 m, with a standard deviation of 0.51 m. These results reveal a low persistence of discontinuities, suggesting that the discontinuities have limited extension at the studied sites.

## 5 Conclusion

The objective of this research is to evaluate the state of fracturing at two sites in the urban area of Meknes using the Scanline survey. This simple and effective approach delivers valuable results. The discontinuity analysis revealed a simple structure, grouped into three main sets oriented N45, N80, and N110, with subvertical dips. These orientations are consistent with regional fracturing.

The distribution of spacing, aperture, and persistence of discontinuities follows a negative exponential law, indicating a random distribution. The majority of discontinuities is closed or has small apertures, generally without filling. However, in some cases, silt and red soil

have been observed. These results will help improve stability risk management, to assess the vulnerability of the area, and preserve local infrastructure.

**Acknowledgment:** We sincerely acknowledge the Geoprospection and Geotechnics Research Team for providing the measuring equipment and its accessories.

**Disclosure of Interests:** The authors declare that they have no competing interests related to the content of this manuscript.

## References

1. Waltham AC, Fookes PG. Engineering classification of karst ground conditions. *Mai* 2003.<https://doi.org/10.1144/1470-9236/2002-33>.
2. Piteau DR, Martin DC. Slope stability analysis and design based on probability techniques at Cassiar Mine. *CIM Bulletin*. 1977;70(779):139-50.
3. Rouai M, Dekayir A, Qarqori K. Slope Stability and Landslide Hazard in Volubilis Archaeo-logical Site (Morocco). In: Guzzetti F, Mihalić Arbanas S, Reichenbach P, Sassa K, Bobrowsky PT, Takara K, éditeurs. *Understanding and Reducing Landslide Disaster Risk 1*. [https://doi.org/10.1007/978-3-030-60227-7\\_43](https://doi.org/10.1007/978-3-030-60227-7_43).
4. Marrett R. Aggregate properties of fracture populations. *Journal of Structural Geology*. 1996,[https://doi.org/10.1016/S0191-8141\(96\)80042-3](https://doi.org/10.1016/S0191-8141(96)80042-3).
5. Priest SD, Hudson JA. Estimation of discontinuity spacing and trace length using scanline surveys. In: *International Journal of Rock Mechanics and Mining Sciences & Geomechanics, Abstracts*, Elsevier, 1981, p. 183-197. [https://doi.org/10.1016/0148-9062\(81\)90973-6](https://doi.org/10.1016/0148-9062(81)90973-6)
6. Faugères JC. Les Rides sud-rifaines: Evolution sédimentaire et structurale d'un bassin atlanti-co-mesogéen de la marge africaine. 1978.
7. Martin J. Le Moyen Atlas central, étude géomorphologique. 1981
8. Cirac P. Le bassin sud-rifain occidental au néogène supérieur: évolution de la dynamique sédimentaire et de la paléogéographie au cours d'une phase de comblement, PhD Thesis, Bordeaux 1; 1985.
9. Essaied A, Rouai M, Dekayir A, Bouhali K. Study of the mechanical behavior of marls: Case from Fes-Meknes region (Morocco). In: *E3S Web of Conferences*. EDP Sciences; 2023. p. 02004. <https://doi.org/10.1051/e3sconf/202336402004>.
10. Taltasse P. Recherches géologiques et hydrogéologiques dans le Bassin lacustre de Fès-Moknès, &c. 1953.
11. Morley CK. A classification of thrust fronts. *AAPG Bulletin*. 1986.
12. Charrière A. Héritage hercynien et évolution géodynamique alpine d'une chaîne intracontinen-tale: Le Moyen-Atlas au SE de Fes (Maroc) PhD Thesis, Toulouse, 1990.
13. Boumir K. Paléoenvironnements de dépôt et transformations post-sédimentaires des sables fauves du bassin du saïs (Maroc) PhD Thesis. Université Henri Poincaré-Nancy 1; 1990
14. Essaied, A., Rouai, M., Dekayir, A., Bouhali, K., 2025. Microzonation and classification of seismic sites based on analysis and modeling of the HVSR data in the city of Meknes, Morocco. <https://doi.org/10.1016/j.soildyn.2025.109451>
15. Hantz D, Rossetti JP, Valette D, Bourrier F. Quantitative rockfall hazard assessment at the Mont Saint-Eynard (French Alps). In: *6th Interdisciplinary Workshop on Rockfall Protection*, 2017.<https://insu.hal.science/insu-03598733/>

16. Priest SD. Discontinuity analysis for rock engineering [Internet]. Springer Science & Busi-ness Media; 1993.
17. Matheron G. Le krigeage universel. Vol. 1. École nationale supérieure des mines de Paris Paris; 1969.<https://doi.org/10.1016/j.geoderma.2003.08.018>.
18. LaPointe PR, Hudson JA. Characterization and interpretation of rock mass joint patterns. Geol Soc Am Spec Pap 199: 1–38. 1985.
19. Cirac P. Le bassin sud-rifain occidental au néogène supérieur: évolution de la dynamique sédimentaire et de la paléogéographie au cours d'une phase de comblement, PPhD Thesis, Bordeaux 1; 1985.
20. Hudson JA, Priest SD. Discontinuities and rock mass geometry. In: International Journal of Rock Mechanics and Mining Sciences & Geomechanics Abstracts. Elsevier; 1979, [https://doi.org/10.1016/0148-9062\(79\)90001-9](https://doi.org/10.1016/0148-9062(79)90001-9).